Available online at www.sciencedirect.com
SCIENCE DIRECT®
Journal of Inorganic Biochemistry 99 (2005) 949–958
JOURNAL OF Inorganic Biochemistry
www.elsevier.com/locate/jinorgbio

# A theoretical study on the binding of $O_2$, NO and CO to heme proteins

L. Mattias Blomberg *, Margareta R.A. Blomberg, Per E.M. Siegbahn

*Department of Physics, Stockholm University, SE-106 91 Stockholm, Sweden*

Received 8 January 2005; received in revised form 2 February 2005; accepted 14 February 2005
Available online 13 March 2005

**Abstract**

The hybrid density functional B3LYP is used to describe the bonding of the diatomic molecules $O_2$, NO and CO to ferrous heme. Three different models are used, a five-coordinated porphyrin in benzene, the myoglobin active site including the distal histidine and the binuclear center in cytochrome oxidase. The geometric and electronic structures are well described by the B3LYP functional, while experimental binding energies are more difficult to reproduce. It is found that the $Cu_B$ center in cytochrome oxidase has a similar effect on the binding of the diatomics as the distal histidine in myoglobin.


*Keywords:* $O_2$; NO; CO; Heme; Myoglobin; Cytochrome oxidase; DFT; B3LYP

## 1. Introduction

Enzymes normally recognize substrates by their shape and polarity. This is, however, very difficult in the case of the diatomic molecules $O_2$, NO and CO, since they are very similar in this respect. The mechanism of discrimination between these molecules is especially important for dioxygen binding enzymes in the respiratory chain, since these enzymes must favor the binding of dioxygen compared to both nitric oxide and carbon monoxide to avoid suffocation. Both NO and CO have a high affinity for ferrous iron. NO binds rapidly both to iron ions in solution and to iron complexes in enzymes, such as iron–sulfur clusters and heme groups [1]. In the present study the binding of these diatomic molecules to two important proteins, cytochrome oxidase and myoglobin, will be discussed.

Cytochrome oxidase is the terminal enzyme in the respiratory chain catalyzing the reduction of dioxygen to water. This exergonic reaction is coupled to the translocation of protons across the mitochondrial inner membrane and the redox energy is converted into the proton motive force, which drives the synthesis of ATP. Four redox active metal centers are present in the enzyme. The electron, coming from the substrate cytochrome *c* in eukaryotes, enters at $Cu_A$ and goes via heme *a* to the binuclear center, heme $a_3$-$Cu_B$, where it is used in the reduction of $O_2$.

The main event in the catalytic cycle of cytochrome oxidase is the cleavage of the O–O bond. Molecular oxygen coordinates to the ferrous heme in the reduced form of the binuclear center, forming the spectroscopically characterized compound **A**. The mechanism for the O–O bond cleavage step has been studied theoretically [2,3] (M.R.A. Blomberg and P.E.M. Siegbahn, to be published), and the calculations indicate that only with an extra positive charge (proton) present in or close to the binuclear center the barrier is low enough to agree with the experimental life time of compound **A**. The most important, but also the most difficult problem of cytochrome oxidase, is the mechanism of the proton

* Corresponding author. Tel.: +46855378706; fax: +46855378601.
*E-mail address:* mattiasb@physto.se (L.M. Blomberg).

0162-0134/$ - see front matter © 2005 Elsevier Inc. All rights reserved.
doi:10.1016/j.jinorgbio.2005.02.014

translocation. In particular, it is difficult to understand how the protons can be allowed to move across the membrane against the gradient potential, but must not be allowed to move the other way, which is thermodynamically more favorable. Several suggestions have been made [4–11], and the general view has been that there must be a pathway that is open at certain occasions and closed at others. This has been termed proton gating. Theoretical studies have suggested a different approach, where the protons are thermodynamically guided towards a proton pumping site [12] (M.R.A. Blomberg and P.E.M. Siegbahn, to be published).

Even though dioxygen is the natural substrate, NO is known to inhibit cytochrome *c* oxidase reversibly by competing with $O_2$ for the binuclear center binding site. At high concentrations, long exposure times or after conversion of NO to one of its oxides like peroxynitrite, the respiratory chain is irreversibly inhibited. It has been shown that NO actually can be reduced by some heme-copper oxidases, such as the cytochrome $ba_3$- and cytochrome $caa_3$-type oxidases in *Thermus thermophilus* [13], cytochrome $cbb_3$ type oxidase of *Paracoccus stutzeri* [14] and also by the quinol $bo_3$ oxidase in *Escherichia coli* [15]. The inhibition of cytochrome oxidase by NO can be the explanation for the observed lower $K_M$ for $O_2$ in whole cells compared to isolated mitochondria [16], and it has been suggested that the NO concentration in mitochondria controls the respiration rate. The fact that CO binds strongly to Fe(II) is used in experiments on cytochrome oxidases to trap the enzyme in the fully reduced state. After adding the dioxygen substrate, the CO molecule is flashed off, and the reaction starting from the fully reduced state can be studied.

Myoglobin (Mb) is a small monomeric enzyme closely related to hemoglobin, the $O_2$ carrier in red blood cells. Mb, which binds molecular oxygen reversibly, is known to work both as a dioxygen storage and as a facilitator of the diffusion of $O_2$ from the capillaries to the mitochondria. Mb contains one heme active site responsible for the $O_2$ binding. The heme iron is coordinated to a proximal histidine (His93) making the iron five coordinated with a free binding site for dioxygen. Above the free binding site a so called distal histidine (His64) is located, which can form a hydrogen bond to the sixth iron ligand. One of the key features of the distal histidine is to discern between $O_2$, NO and CO, favoring $O_2$ by mainly electrostatic interactions [17]. Without the distal histidine the low concentration of CO produced by different catabolic processes in the body would inhibit the enzyme and lead to suffocation.

In the past decades the importance of NO working as an intercellular messenger molecule regulating a number of physiological functions has been discovered. In eukaryotic cells NO is produced by nitric oxide synthase (NOS) which uses the substrates $O_2$ and arginine. One of the degradation routes for NO is the reaction of NO with hemoglobin [18]. As mentioned above, NO is also known to inhibit important enzymatic processes, and furthermore it is involved in the oxidation and nitration processes, that damage proteins [19,20] and DNA [21]. NO reacts at almost diffusion controlled rate with superoxide forming peroxynitrite [22], and peroxynitrite, in turn, is believed to be responsible for the nitrating and oxidative damage observed at high NO concentrations. This reaction led to the suggestion that, due to the superoxide character of heme bound $O_2$, NO could react with oxy-Mb. The reaction mechanism for this process has been investigated in a theoretical study, showing that the reaction between NO and oxy-Mb leads to a short-lived peroxynitrite intermediate coordinated to a ferric heme iron. The O–O bond in peroxynitrite is broken homolytically forming an $NO_2$-radical, and the heme is oxidized to oxo-Fe(IV). The $NO_2$-radical attacks the Fe(IV)=O in a rebound type of mechanism forming nitrate. All the reaction steps have low barriers showing that the reaction between NO and oxy-Mb should be an efficient way of scavenging NO [23].

NO is also the substrate of the nitric oxide reductase (NOR) which is a part of the denitrification chain. At low dioxygen levels, insufficient to use $O_2$ as the electron acceptor in respiration, anaerobic bacteria can use $NO_3^-$ to produce ATP in a similar way. Nitric oxide reductase is a part of this chain of enzymes reducing nitrate. NOR and cytochrome oxidase are believed to have a common ancestor and have similar structures. One of the major differences is in the binuclear center, consisting of an Fe–$Cu_B$ center in cytochrome oxidases, while in NOR $Cu_B$ is exchanged by a non-heme iron. Some cytochrome oxidases show NOR activity, and the mechanism for the reduction of two equivalents of NO to nitrous oxide ($N_2O$) and water in a $ba_3$-type of heme-copper oxidase has been investigated theoretically (L.M. Blomberg, M.R.A. Blomberg and P.E.M. Siegbahn, to be published). The corresponding reduction of NO in NOR is furthermore under investigation (L.M. Blomberg, M.R.A. Blomberg and P.E.M. Siegbahn).

Numerous different porphyrins have been synthesized, and since the most common axial ligand coordinating to heme groups in enzymes is histidine, the synthetic porphyrins often have an imidazole coordinating to the iron. These model porphyrins have been used experimentally to gain more knowledge about the properties and functioning of heme groups in enzymes. Among other things the binding of small diatomics has been studied [17].

The binding of $O_2$, NO and CO to heme iron is of great importance, since this binding is either the initiation of the chemical reactions described above, or the inhibition of those reactions, and a thorough investigation of the binding properties of these diatomic molecules is needed. Below some results from density

functional studies of the binding of $O_2$, NO and CO to different heme models are summarized. The three models used are a pure five coordinated porphyrin, the heme binding site in myoglobin including the distal histidine, and the binuclear center in cytochrome oxidase. In this way also the effects of the surroundings on the ligand binding are explored.

## 2. Model

In the present study the crystal structure of a $ba_3$-type heme-copper oxidase [24] of the prokaryote *T. thermophilus* has been used as a starting point modeling the active site of a cytochrome oxidase, see Fig. 1. Furthermore, the crystal structure of horse heart myoglobin [25] was used as a starting point modeling the active site of myoglobin, see Fig. 2.

The overall structure surrounding the binuclear center ($a_3$-$Cu_B$) in the $ba_3$-type oxidase is very similar to the $aa_3$-type in mammals (bovine heart) and bacteria *Paracoccus denitrificans* and *Rhodobactor sphaeroides*. $Cu_B$ is coordinated to three histidines, His282, His283 and His233, where His233 is covalently bound to Tyr237. Heme $a_3$ is coordinated to His384 and propionate A is hydrogen bonding to His376 and Asp372 and propionate D to Arg449, see Fig. 1.

In the present study the heme group is always modeled as a porphyrin ring without substituents. In the model of the cytochrome oxidase active site the proximal His384 is modeled as a 4-ethylimidazole with the α-carbon of the histidine frozen. His233 is modeled as a 1-methyl-4-ethyl-imidazole with the α-carbon and the Tyr237 meta-carbon frozen. The two adjacent His282 and His283 and the backbone between them are incorporated into the model with the peptide nitrogen frozen. All frozen coordinates are taken from the crystal structure.

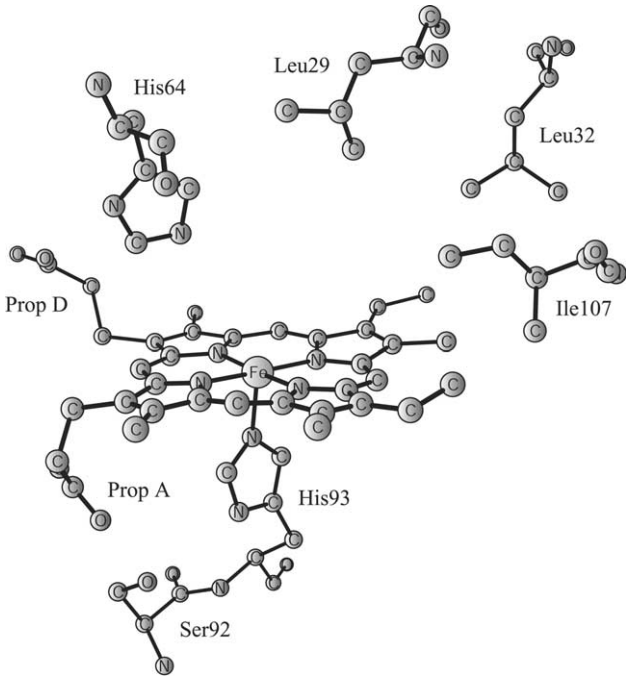


Fig. 2. The active site of the horse heart myoglobin.

In the model of the myoglobin active site the proximal histidine is modeled as ammonia which is a well

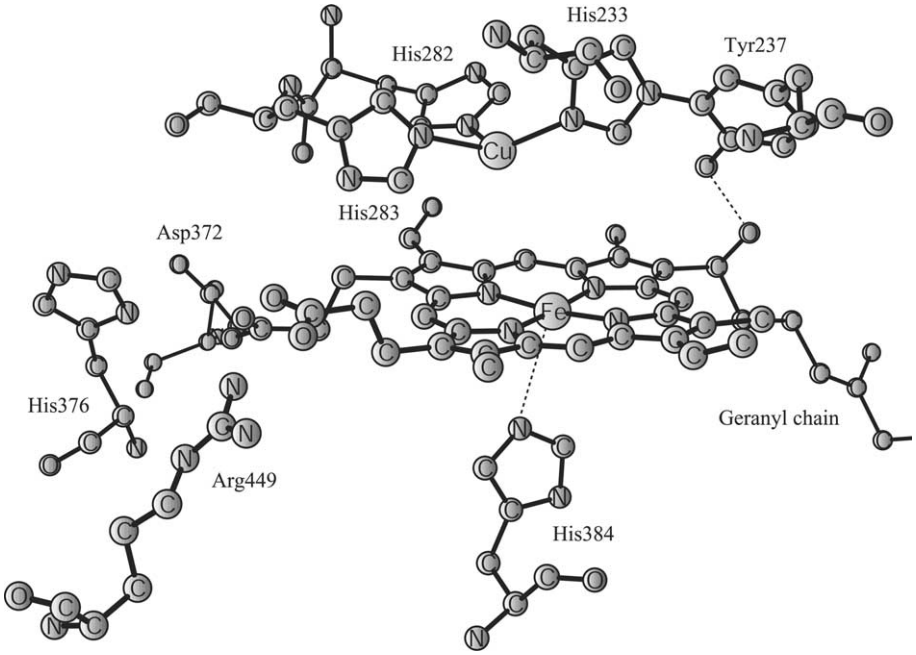


Fig. 1. The binuclear active site of the $ba_3$-type of oxidase in *Thermus thermophilus*.

tested model of imidazoles coordinated to heme. The distal histidine is modeled as a 4-ethylimidazole with the α-carbon frozen according to the crystal structure. The five coordinated porphyrin model is identical to the model of myoglobin omitting the distal histidine.

## 3. Methods

The geometries were optimized using Becke's [26] three parameter hybrid exchange functional combined with the Lee–Yang–Parr [27] correlation functional (B3LYP). The calculations were performed using the Gaussian 03 [28] and Jaguar [29] programs. The geometries were optimized with the lacvp double-ζ quality basis set implemented in JAGUAR [29], with an effective core potential (ECP) on iron and copper. The open shell systems were treated using unrestricted B3LYP.

The final energies for the optimized geometries were evaluated using the B3LYP functional and the lacv3p**+ basis set of JAGUAR, which is a triple-ζ basis set with ECP on the metals and includes one diffuse function on the heavy atoms and one polarization function on all atoms except on the metal ions. For iron an f-function was included in the calculations on the small porphyrin model. The effect of the f-function on the binding energy of $O_2$, NO and CO, respectively, was used to correct the corresponding binding energies in the models of myoglobin and cytochrome oxidase. The dielectric effects from the surrounding environment were obtained for all stationary points using the Jaguar self-consistent reaction field method [30] using the lacv3p**+ basis set for the porphyrin and myoglobin models and the lacvp basis set for the cytochrome oxidase model. In the active site models of myoglobin and cytochrome oxidase the dielectric constant was set equal to four, which corresponds to a dielectric constant of about three for the protein and 80 for the water medium surrounding the protein [31]. The probe radius of the solvent was set to 1.4 Å, which corresponds to a water molecule. In the model porphyrin experiments benzene was used as solvent, and therefore, in the calculations on the pure porphyrin model the dielectric constant was set equal to 2.28 and the probe radius was 2.60 Å.

Density functional theory (DFT) does not describe low spin open-shell systems correctly, but the too high energy of the low-spin state can be corrected by calculating also the state with the highest $M_S$ value. A $J$-value can then be obtained using the Heisenberg Hamiltonian formalism [32]. In the present study, dioxygen bound to the ferrous heme iron is known to be an open shell singlet, which is reproduced in the calculations. In the singlet–triplet case the $J$-value corresponds to twice the calculated energy difference between the triplet and open-shell singlet (broken symmetry) states. In the present study the calculated $J$-value for the porphyrin, myoglobin and cytochrome oxidase models are 5.0, 10.1 and 6.0 kcal/mol, respectively. All Fe(II)-$O_2$ energies are corrected by subtracting $J/2$ from the calculated open-shell singlet energies.

The accuracy of the B3LYP functional has been tested in the extended G3 benchmark set [33], which consists of enthalpies of formation, ionization potentials, electron affinities and proton affinities for molecules containing first- and second-row atoms. The B3LYP functional gives an average error of 4.3 kcal/mol [33] for 376 different molecules. Due to the lack of accurate experimental data for transition metals there are few benchmark tests. Normal metal–ligand bond strengths indicate that the errors are slightly larger, 3–5 kcal/mol [34]. Different aspects of modeling enzyme active sites are described in recent reviews [35,36].

The relative energies discussed below are Gibb's free energies with the solvent effects included. However, due to the freezing of certain structural parameters, entropy effects could not be obtained from Hessian calculations, and therefore a standard $\Delta\Delta G$ correction of 10 kcal/mol for the binding of a diatomic molecule is used.

## 4. Results

The high affinity of Fe(II) for NO and CO makes them potent inhibitors for all ferrous heme iron enzymes and the discrimination between $O_2$ on one side and NO and CO on the other is of great importance for all ferrous iron enzymes binding dioxygen. The binding of $O_2$, NO and CO to ferrous porphyrin systems have been studied extensively both experimentally [17–40] and theoretically [40–47]. Compared to the earlier theoretical studies the present investigation is extended by incorporating the binding of NO in myoglobin and all three diatomic ligands in cytochrome oxidase. The binding energies and structural features are compared between the models and the influence of the distal side of the heme is discussed.

### 4.1. Coordination of $O_2$, NO and CO to the porphyrin, myoglobin and cytochrome oxidase

Dioxygen is known to form the weakest bond to ferrous iron among the three studied diatomic molecules. The bent geometry can be explained by a favorable interaction between the π*-orbital of the dioxygen and the $d_{z^2}$-orbital on the iron [48]. The π*-orbital of dioxygen is closer in energy to the iron $d_{z^2}$-orbital compared to the π*-orbitals in iron bound NO and CO, and therefore it gains more energy by bending, which increases the overlap. The structure of $O_2$ bound to the ferrous heme iron in the three models are shown in Figs. 3(a), 4(a) and 5.

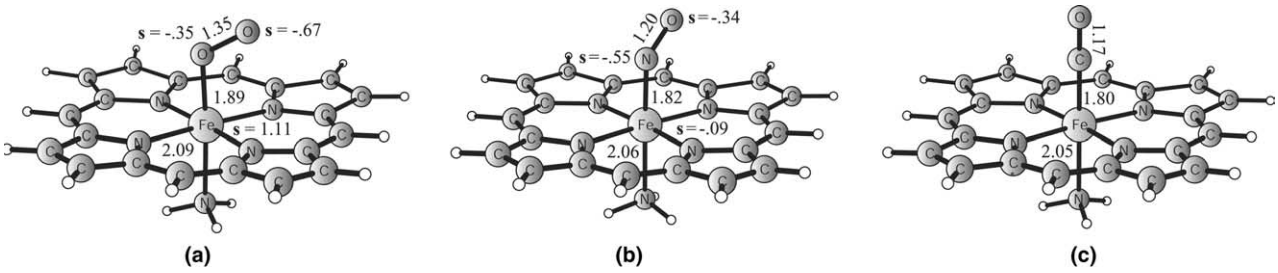


Fig. 3. (a) The binding of molecular oxygen, (b) nitric oxide and (c) carbon monoxide to a five coordinated porphyrin.

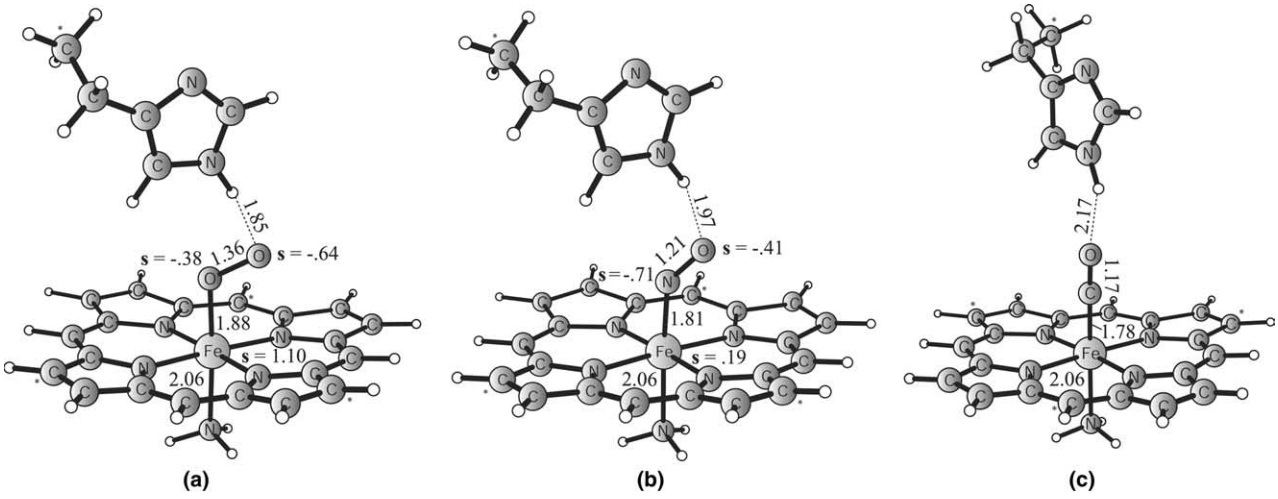


Fig. 4. (a) The binding of molecular oxygen, (b) nitric oxide and (c) carbon monoxide to the myoglobin active site.

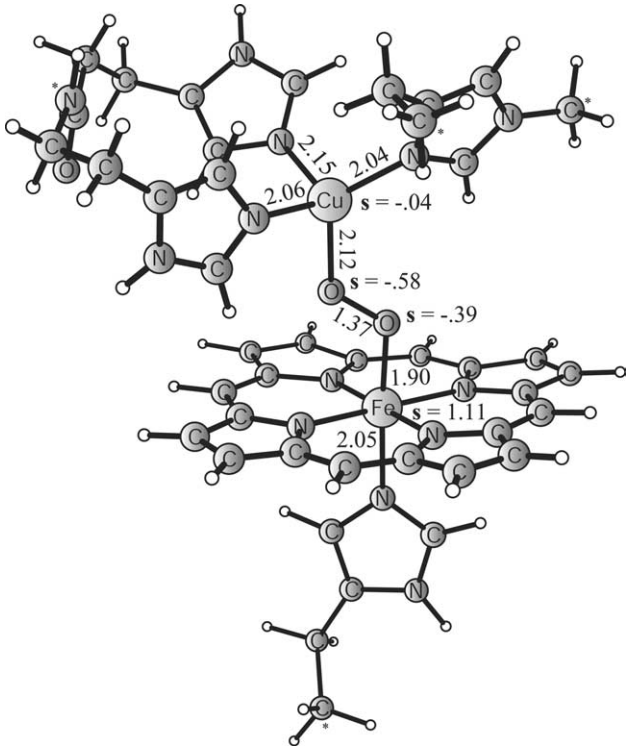


Fig. 5. The binding of molecular oxygen in the binuclear center.

The differences in bond distances, angles and spin distributions are very small for the three different models, see Table 1. The Fe–$O_2$ bond distance varies only slightly from 1.88 to 1.90 Å and similarly the changes in the Fe–O–O angle are small (116–118°). The O–O bond distance varies between 1.35 and 1.37 Å. Molecular oxygen coordinated to a heme iron has an O–O bond length in between dioxygen and peroxide and can be regarded as a superoxide coordinated to a ferric iron. The spin distribution clearly shows that the iron is oxidized to a low spin Fe(III) which is antiferromagnetically coupled to the unpaired electron located on the two oxygens of superoxide. The main difference for the investigated model systems is the spin population on the primary oxygen which decreases from −0.68 in porphyrin to −0.64 and −0.58 in myoglobin and cytochrome oxidase, respectively. The charge on the $O_2$-moiety is small in all the models used in the present study and thus also the difference between them, see Table 1. The tabulated values are from the gas phase calculation, and when a dielectric medium is included the negative charge on $O_2$ increases slightly, the largest value being −0.21. The hydrogen bond in Mb and the electrostatic interaction with $Cu_B$ seems to have similar effects on the electronic structure of heme bound $O_2$ increasing the spin on the primary oxygen slightly.

Table 1
Structural parameters, charge and spin populations of $O_2$ binding to porphyrin, myoglobin and cytochrome oxidase

| | Porphyrin | Myoglobin | Cytochrome oxidase |
|---|---|---|---|
| $r(O_2\cdots His/O_2\cdots Cu_B)$ (Å) | – | 1.85 | 2.12 |
| $r$(Fe–O) (Å) | 1.89 | 1.88 | 1.90 |
| $r$(O–O) (Å) | 1.35 | 1.36 | 1.37 |
| $a$(Fe–O–O) | 118.1° | 116.6° | 117.3° |
| Mulliken charge $O_2$ | −0.09 | −0.15 | 0.05 |
| Mulliken spin population (Fe) | 1.12 | 1.10 | 1.11 |
| Mulliken spin population (O (2°)) | −0.35 | −0.38 | −0.39 |
| Mulliken spin population (O (1°)) | −0.68 | −0.64 | −0.58 |

Table 2
Structural parameters, charge and spin populations of NO binding to porphyrin, myoglobin and cytochrome oxidase

| | Porphyrin | Myoglobin | Cytochrome oxidase |
|---|---|---|---|
| $r(NO\cdots His/NO\cdots Cu_B)$ (Å) | – | 1.97 | 2.41 |
| $r$(Fe–N) (Å) | 1.82 | 1.81 | 1.81 |
| $r$(N–O) (Å) | 1.20 | 1.21 | 1.22 |
| $a$(Fe–N–O) | 142.0° | 138.1° | 140.4° |
| Mulliken charge NO | −0.06 | −0.11 | 0.05 |
| Mulliken spin population (Fe) | −0.05 | 0.19 | 0.30 |
| Mulliken spin population (N) | −0.58 | −0.71 | −0.76 |
| Mulliken spin population (O) | −0.34 | −0.41 | −0.45 |

Nitric oxide bound to ferrous heme also has a bent structure, but here the angle is larger since the energy of its π*-orbital differs compared to the $d_{z^2}$-orbital on iron, decreasing the stabilization gained by increasing the overlap, see Figs. 3(b), 4(b) and 6. The angle is increased from 116-118° for heme bound $O_2$ to 138–142° for NO, see Tables 1 and 2. Similarly to the structural changes of the $O_2$ coordination in the different models, the changes in the geometry of the coordinated NO are minor, see Table 2. The charge on the NO-moiety is also very small, and changes only slightly between the models of myoglobin and cytochrome oxidase. The incorporation of the distal histidine in myoglobin and $Cu_B$ in cytochrome oxidase increases the oxidation of the heme iron and reduces NO to more $NO^-$ character. From being essentially not oxidized at all in the porphyrin model the spin population on iron increases to 0.19 in myoglobin and 0.30 in cytochrome oxidase. The oxidation of the ferrous iron to a more ferric state reduces NO and the spin on both the nitrogen and oxygen increases from −0.58 and −0.34 in the porphyrin model to more triplet character with a spin population of −0.76 and −0.45 in the cytochrome oxidase model, see Table 2.

In contrast to $O_2$ and NO, CO has an almost straight geometry in all models, see Figs. 3(c), 4(c) and 7 and Table 3. The difference in energy between the π*-orbital

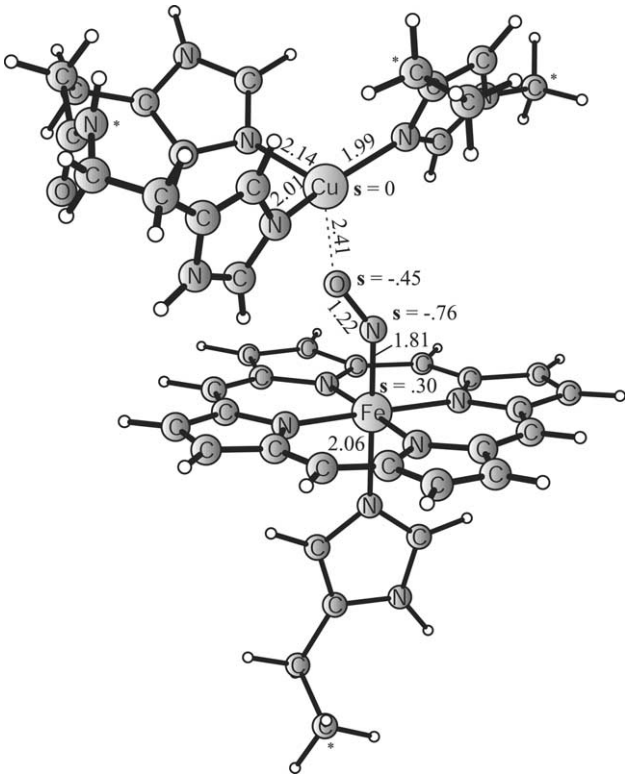


Fig. 6. The binding of nitric oxide in the binuclear center.

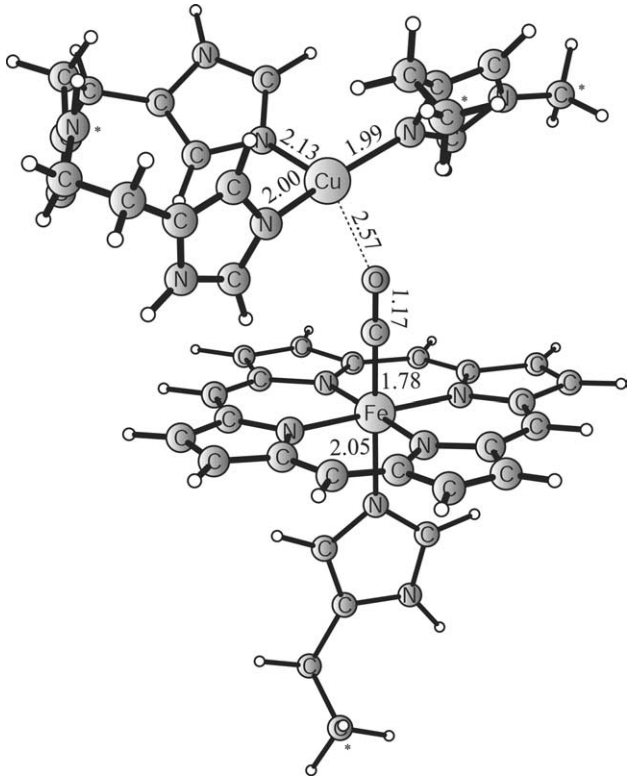


Fig. 7. The binding of carbon monoxide in the binuclear center.

Table 3
Structural parameters, charge and spin populations of CO binding to porphyrin, myoglobin and cytochrome oxidase

| | Porphyrin | Myoglobin | Cytochrome oxidase |
|---|---|---|---|
| $r$(CO···His/CO···$Cu_B$) (Å) | – | 2.17 | 2.57 |
| $r$(Fe–C) (Å) | 1.80 | 1.78 | 1.78 |
| $r$(C–O) (Å) | 1.17 | 1.17 | 1.17 |
| $a$(Fe–C–O) | 179.9° | 176.2° | 179.6° |
| Mulliken charge CO | −0.18 | −0.15 | 0.01 |

of CO and the $d_z^2$-orbital of iron is larger than for NO and $O_2$ and there is no stabilization gained by bending [48]. The distal side of the heme has almost no effect on the bond distances and angles of CO. The Fe–C bond distance varies between 1.78 and 1.80 Å and the C–O bond distance does not change (1.17 Å). The Fe–C–O angle varies in the range 176–180°. The charge on the CO-moiety is small and hardly changes in the different models, see Table 3.

The general picture given above for the binding of $O_2$, NO and CO to hemes is in good agreement with experimental information as well as with previous theoretical studies [42,43,40,41,45–47]. One exception is a recent study where the picture of the binding obtained by B3LYP was compared to the one given by CASSCF, which is an ab initio method capable of handling near degeneracy effects [44]. It was concluded that B3LYP fails to give the correct picture of the binding of $O_2$ to a porphyrin complex. However, this conclusion has been revised in an erratum in the present issue [49].

### 4.2. Binding energies of $O_2$, NO and CO in porphyrin, myoglobin and cytochrome oxidase

Whereas the general picture of the bonding and structure for $O_2$, NO and CO to the ferrous heme was relatively easily obtained with satisfactory results, the situation for the bond dissociation energies turned out to be much more difficult. Surprisingly large deviations to experimental trends were in fact obtained. It must in this context be remembered that a comparison between calculated and experimental energies is far from straightforward but requires several assumptions, see below. The calculated Gibbs free energies of binding to the ferrous heme in porphyrin, myoglobin and cytochrome oxidase are listed in Table 4. The binuclear center in cytochrome oxidase is in its fully reduced state Fe(II)–$Cu_B$(I).

Table 4
Calculated Gibbs free energy of binding for $O_2$, NO and CO in porphyrin, myoglobin and cytochrome oxidase

| | Fe–$O_2$ (kcal/mol) | Fe–NO (kcal/mol) | Fe–CO (kcal/mol) |
|---|---|---|---|
| Porphyrin | 2.4 | −2.5 | −6.9 |
| Myoglobin | −8.1 | −2.8 | −6.2 |
| Cytochrome oxidase | −4.1 | −1.3 | −4.2 |

To be able to compare the computed binding energies with experimental results the experimental data have been analyzed. The many studies made on both heme enzymes and porphyrin model systems give several experimental results to which the calculated binding energies can be compared. From dissociation rate constants of the diatomic ligands, dissociation barriers can be calculated using transition state theory. Dissociation barriers for the ligands $O_2$, NO and CO are listed in Table 5 for the systems where experimental data are available. Experimental equilibrium constants can be used to calculate relative binding energies. Both the relative binding energy for different ligands in the same system and for the same ligand in different systems can be evaluated. For example, the ratio of the equilibrium constants for CO and $O_2$ in myoglobin is $K_{CO}/K_{O_2} = 25$, which means that CO binds 1.9 kcal/mol stronger than $O_2$ in ferrous myoglobin. These types of relative binding energies are listed in Table 6. In the same way the relative binding energies for the same ligand in different systems can be evaluated, see Table 7.

A rough value of the absolute binding energies for the ligands can be obtained from the experimental dissociation barriers by assuming that the barriers for the association of the diatomic molecules are similar for all ligands and systems. The similar size and polarity of the three diatomic molecules support this assumption at a qualitative level. Another assumption is that the height of the association barriers is estimated to be around 10 kcal/mol, which corresponds to the rough loss of entropy when binding a diatomic molecule. The loss of entropy in the transition state for the binding of a diatomic molecule with a low enthalpy barrier has in previous theoretical studies been shown to be similar to the entropy loss for the bound molecule [50,23]. Thus, by subtracting 10 kcal/mol from the dissociation barriers a rough estimate of the absolute binding energy of the diatomic ligands is obtained, see Table 5. A way of testing the assumption that the association barriers are similar for all three ligands in the different systems is to use the binding energies obtained to calculate the relative values, and compare them with the relative binding

Table 5
Experimental dissociation barriers and estimated binding energies for $O_2$, NO and CO [17,38]

| | Dissoc. barrier | | | Estimated bind. $\Delta G$[b] | | |
|---|---|---|---|---|---|---|
| | $O_2$ | NO | CO | $O_2$ | NO | CO |
| Chelated protoheme[a] | 12.3 | – | – | −2.3 | – | – |
| Myoglobin | 16.1 | 22.8 | 18.5 | −6.1 | −12.8 | −8.5 |
| Cytochrome oxidase | – | 18.7 | 19.7 | – | −8.7 | −9.7 |

[a] Mono-3-(1-imidazoyl)-propylamide monomethyl ester.
[b] Calculated from the dissociation barriers by assuming that the barrier for binding the ligands to the heme iron is 10 kcal/mol.

Table 6
Relative binding energies comparing the molecules $O_2$, NO and CO

| | Expr. rel. bind. $\Delta G$ | | | Calc. rel. bind. $\Delta G$ | | |
|---|---|---|---|---|---|---|
| | $CO/O_2$ | $NO/O_2$ | NO/CO | $CO/O_2$ | $NO/O_2$ | NO/CO |
| Chelated protoheme[a] | −5.8 | – | – | −9.3 | −4.9 | +4.4 |
| Myoglobin | −1.9 | −7.1 | −5.2 | +1.9 | +5.3 | +3.4 |
| Cytochrome oxidase | – | – | −3.2 | +0.1 | +2.8 | +2.9 |

The experimental relative binding energies are calculated from equilibrium constants.
[a] Mono-3-(1-imidazoyl)-propylamide monomethyl ester.

Table 7
Relative binding energies in porphyrin, myoglobin and cytochrome oxidase for each of the molecules $O_2$, NO and CO

| | Relative binding energies | | | |
|---|---|---|---|---|
| | Myoglobin/porphyrin | | Myoglobin/cytochrome oxidase | |
| | Expr. | Calc. | Expr. | Calc. |
| $O_2$ | −2.5 | −10.5 | – | −4.0 |
| NO | ±1[a] | −0.3 | −3.0 | −1.5 |
| CO | +1.5 | +0.7 | +0.1 | −2.0 |

[a] Relative binding energy of NO in apolar distal histidine mutants.

energies calculated from the equilibrium constants. In most cases these relative binding energies differ by only 1 kcal/mol from each other. However, cytochrome oxidase is an exception, where the relative bond strength for NO/CO calculated from the equilibrium constants is −3.2 kcal/mol, whereas the corresponding value calculated from the approximate experimental bond strengths listed in Table 6 is +1.0 kcal/mol. This result indicates that the barrier for binding CO in cytochrome oxidase should be higher than the corresponding barrier for binding NO and it also implies that the binding energy of CO in cytochrome oxidase in Table 5 could be overestimated.

Comparing the estimated experimental values for the Gibbs free energy of binding with the calculated values shows that the calculated binding energies for $O_2$ and CO deviates by less than 6 kcal/mol from the experimental values, while the bond strength of NO deviates with 8–11 kcal/mol, see Tables 4 and 5. Note that the same entropy correction is used both to estimate the experimental binding energies and correcting the calculated binding energies. This makes the comparison less sensitive to the choice of the size of the correction as long as the assumption that the difference in entropy between the transition state and the bound state is small. In a previous study Rovira et al. [43] calculated the bond strengths of $O_2$, NO and CO to a porphyrin model very similar to the one used in the present study. Their calculated enthalpy bond strengths are 15, 36 and 35 kcal/mol for $O_2$, NO and CO, respectively. Adding the approximative entropy loss for binding diatomic molecules, the Gibbs free energies of binding would be −5, −26 and −25 kcal/mol for $O_2$, NO and CO, respectively. These results can be compared to the corresponding values obtained for the porphyrin model in the present study, which are 2.4, −2.5 and −6.9 kcal/mol for $O_2$, NO and CO, respectively (Table 4), showing the extreme sensitivity to the choice of DFT method. Rovira et al. [43] used a gradient corrected density functional without Hartree–Fock exchange which is known to give too large binding energies for metal–ligand bonds [34]. In the present study, a hybrid density functional have been used which instead can be expected to give too small binding energies which is consistent with the fact that van der Waals attraction is missing in DFT methods. By decreasing the amount of Hartree–Fock exchange the metal–ligand bond strength increases, and the bond strength difference between NO and CO decreases indicating that an interpolation to a non-hybrid DFT method would go towards the results of Rovira et al. [43].

The relative binding energies of $O_2$, NO and CO to ferrous iron are of large importance since it is the difference in bond strength that discriminates between the diatomic molecules. The binding energy for $O_2$ is known to vary depending on the polarity of the Fe–$O_2$ moiety surroundings, while NO and CO are much less affected. The binding of $O_2$ and CO to myoglobin have been studied both experimentally and theoretically showing that hydrogen bonding to the distal histidine stabilizes $O_2$ bound to the ferrous iron more than CO which is crucial for favoring the binding of $O_2$. The relative equilibrium constants $K_{CO}/K_{O_2} = 25$ for myoglobin can be compared with $K_{CO}/K_{O_2} = 22,000$ for a free porphyrin in benzene, which corresponds to a relative change in affinity for $CO/O_2$ of 4.0 kcal/mol, that is the binding of $O_2$ being favored by 4.0 kcal/mol more than CO by the presence of the distal histidine. The calculated effect of

incorporating the distal histidine hydrogen bonding to the heme bound $O_2$ and CO can be seen in Table 7. The calculated relative change in bond strength for CO/$O_2$ is 11.2 kcal/mol. Sigfridsson and Ryde [41] used a very similar model of myoglobin and calculated a corresponding value of 7 kcal/mol. However, the procedures used to calculate the effect of the distal histidine differ between the present study and the one by Sigfridsson and Ryde, and the details of the deviations between the two calculations are under investigation. The presently calculated stabilization of the Fe(II)–$O_2$ moiety by the distal histidine is also overestimated when compared to the experimental effect of 4.0 kcal/mol. The calculated binding energy of CO decreases by 0.7 kcal/mol in the presence of the distal histidine, which is quite similar to the experimental decrease in bond strength of 1.5 kcal/mol [17], see Table 7. The calculated change in binding energy for $O_2$ by incorporating the distal histidine is an increase by 10.5 kcal/mol, thus significantly larger than the experimental increase of 2.5 kcal/mol [17], see Table 7. Since the accuracy of B3LYP for describing a hydrogen bonding effect is expected to be much better than this, the origin of the discrepancy between the calculated and experimental effect is likely due to the chemical model used. A possible explanation could be that before $O_2$ enters, the distal histidine is involved in a hydrogen bond to a group not included in the present model and this bond has to be broken to form the hydrogen bond to $O_2$. Calculations are in progress to investigate this possibility. In the case of NO the calculated binding to the ferrous iron is only stabilized by 1.0 kcal/mol by the presence of the hydrogen bond to the distal histidine in myoglobin. This results fits rather well with the experimental observation that mutating the distal histidine to an apolar amino acid has only minor effects on the equilibrium constant of NO, corresponding to a change in binding energy of $\pm$1 kcal/mol [17], see Table 7.

Comparing the experimental binding energies of $O_2$, NO and CO in myoglobin and cytochrome oxidase, shows that both the absolute bond strengths and the trends between the different ligands are similar for the two systems, see Table 5. This implies that $Cu_B$ stabilizes $O_2$, NO and CO in the same way and to a similar extent as the distal histidine in myoglobin, a trend that is reproduced by the calculations, see Table 4. However, the order in the bond strength of $O_2$, NO and CO cannot be reproduced neither in cytochrome oxidase nor in myoglobin. Consequently, the relative binding energies for the three diatomic ligands deviate surprisingly much from the relative energies calculated from the experimental equilibrium constants. The calculated and experimental relative binding energies are listed in Table 6. Experimentally NO binds 7.1 kcal/mol stronger than $O_2$ to the ferrous iron in myoglobin, whereas CO binds 1.9 kcal/mol stronger than $O_2$. In the calculations on the other hand NO binds 4.5 kcal/mol weaker than $O_2$ to the heme in myoglobin while CO binds 0.5 kcal/mol weaker, see Table 4. Comparing the calculated and experimental relative binding energies in myoglobin shows that the relative bond strengths of $O_2$ and CO are quite well reproduced whereas NO binds too weakly to the heme in myoglobin. The underestimation of the bond strength of NO to the ferrous heme is the largest error compared to the experiments.

The changes in the binding energies for $O_2$, NO and CO between the different systems are quite well reproduced in the calculations as can be seen from Table 7. The largest deviation is for dioxygen where the stabilization by the distal histidine is overestimated, which was discussed above.

## 5. Summary

The binding of the diatomics $O_2$, NO and CO to ferrous heme enzymes is important for the understanding of the mechanisms for discrimination between these diatomic molecules. In the present study the Gibbs free binding energies of $O_2$, NO and CO have been calculated for models of three different system, a free porphyrin in benzene, myoglobin and cytochrome oxidase. The two enzymes are of large importance for respiration and thereby for ATP synthesis. To reproduce the relative binding energies and even the order in bond strengths for these diatomic molecules turned out to be more difficult than expected. The relative bond strengths of $O_2$ and CO are quite well reproduced in the calculations whereas NO binds too weakly. Also the absolute binding energies for CO and $O_2$ are reasonably well reproduced, being 2–5 kcal/mol too small, which is expected since van der Waals interaction is not included in DFT. The largest error compared to the experimental results is obtained for NO, where the underestimation of the bond strength to the ferrous heme is on the order of 10 kcal/mol. At present there is no reasonable explanation for this large error. However, it should be noted that these weak metal ligand bonds are particularly complicated and difficult to describe, in contrast to stronger more covalent types of bonds, where the errors in the calculations have been found to be significantly smaller [51].

The variations in the binding energy of each of the three diatomic molecules between the different model systems are also quite well reproduced compared to experiments, with one important exception. The calculated effect on the binding energy of $O_2$ from the distal histidine in myoglobin is much larger than what is expected from the experimental results. This exaggerated increase in binding energy of $O_2$ might be explained by deficiencies in the myoglobin model used. It may be

necessary to include additional hydrogen bonding groups in the model. The calculations furthermore show that $Cu_B$ in cytochrome oxidase has a similar effect on the binding energies of $O_2$, NO and CO as the distal histidine in myoglobin.

Concerning the binding of $O_2$, NO and CO to ferrous heme enzymes two main problems with the theoretical treatment must be further investigated, these are the too weak bonding of the NO molecule to ferrous heme and the too large effect of the distal histidine on the $O_2$ binding in the myoglobin model.

## Appendix A. Supplementary data

The cartesian coordinates of the structures shown in Figs. 3–7 can be found in the online version at doi:10.1016/j.jinorgbio.2005.02.014.

## References

[1] G.C. Brown, Biochim. Biophys. Acta 1504 (2001) 46–57.
[2] M.R.A. Blomberg, P.E.M. Siegbahn, G.T. Babcock, M. Wikström, J. Am. Chem. Soc. 122 (2000) 12848–12858.
[3] M.R.A. Blomberg, P.E.M. Siegbahn, M. Wikström, Inorg. Chem. 42 (2003) 5231–5243.
[4] J.E. Morgan, M.I. Verkhovsky, M. Wikström, J. Bioenerg. Biomemb. 26 (1994) 599–608.
[5] M. Wikström, J.E. Morgan, M.I. Verkhovsky, J. Bioenerg. Biomemb. 30 (1998) 139–145.
[6] M. Wikström, Biochim. Biophys. Acta 1458 (2000) 188–198.
[7] M. Wikström, M.I. Verkhovsky, G. Hummer, Biochim. Biophys. Acta 1604 (2003) 61–65.
[8] H. Michel, Proc. Natl. Acad. Sci. USA 95 (1998) 12819–12824.
[9] H. Michel, Biochemistry 38 (1999) 15129–15140.
[10] M. Ruitenberg, A. Kannt, E. Bamberg, K. Fendler, H. Michel, Nature 417 (2002) 99–102.
[11] P. Brzezinski, G. Larsson, Biochim. Biophys. Acta 1604 (2003) 61–65.
[12] P.E.M. Siegbahn, M.R.A. Blomberg, L.M. Blomberg, J. Phys. Chem. B 107 (2003) 10946–10955.
[13] A. Giuffrè, G. Stubauer, P. Sarti, M. Brunori, W.G. Zumft, G. Buse, T. Soulimane, Proc. Natl. Acad. Sci. USA 96 (1999) 14718–14723.
[14] E. Forte, A. Urbani, M. Saraste, P. Sarti, M. Brunori, A. Giuffrè, Eur. J. Biochem. 268 (2001) 6486–6490.
[15] C.S. Butler, E. Forte, F.M. Scandurra, M. Arese, A. Giuffrè, C. Greenwood, P. Sarti, Biochem. Biophys. Res. Commun. 296 (2002) 1272–1278.
[16] G.C. Brown, C.E. Cooper, FEBS Lett. 356 (1994) 295–298.
[17] J.S. Olson, G.N. Phillips Jr., J. Biol. Inorg. Chem. 2 (1997) 544–552.
[18] M. Kelm, Biochim. Biophys. Acta 1411 (1999) 273–289.
[19] H. Ischiropoulos, Arch. Biochem. Biophys. 356 (1998) 1–11.
[20] R. Radi, J.S. Beckman, K.M. Bush, B.A. Freeman, J. Biol. Chem. 266 (1991) 4244–4250.
[21] P.A. King, V.E. Anderson, J.O. Edwards, G. Gustafson, R.C. Plumb, J.W. Suggs, J. Am. Chem. Soc. 114 (1992) 5430–5432.
[22] R. Kissner, T. Nauser, P. Bugnon, P.G. Lye, W.H. Koppenol, Chem. Res. Toxicol. 10 (1997) 1285–1292.
[23] L.M. Blomberg, M.R.A. Blomberg, P.E.M. Siegbahn, J. Biol. Inorg. Chem. 9 (2004) 923–935.
[24] T. Soulimane, G. Buse, G.P. Bourenkov, H.D. Bartunik, R. Huber, M.E. Than, EMBO J. 19 (2000) 1766–1776.
[25] R. Maurus, R. Bogumil, N.T. Nguyen, G. Mauk, G. Brayer, Nitric oxide: Biol. Chem. 332 (1998) 67–74.
[26] A.D. Becke, J. Chem. Phys. 98 (1993) 5648–5652.
[27] C. Lee, W. Yang, R.G. Parr, Phys. Rev. B 37 (1988) 785–789.
[28] M.J. Frisch et al., Gaussian 03, Revision B. 03, Gaussian Inc., Pittsburgh, PA, 2003.
[29] Schrödinger, Inc., Portland, Oregon, Jaguar 4.2, 2000.
[30] D.J. Tannor, B. Marten, R. Murphy, R.A. Friesner, D. Sitkoff, A. Nicholls, M. Ringnalda, W.A. Goddard III, B. Honig, J. Am. Chem. Soc. 116 (1994) 11875–11882.
[31] M.R.A. Blomberg, P.E.M. Siegbahn, G.T. Babcock, J. Am. Chem. Soc. 120 (1998) 8812–8824.
[32] L. Noodleman, A.C. Case, Adv. Inorg. Chem. 38 (1992) 423–470.
[33] L.A. Curtiis, K. Raghavachari, R.C. Redfern, J.A. Pople, J. Chem. Phys. 112 (2000) 7374–7383.
[34] P.E.M. Siegbahn, M.R.A. Blomberg, Annu. Rev. Phys. Chem. 50 (1999) 221–249.
[35] P.E.M. Siegbahn, M.R.A. Blomberg, Chem. Rev. 100 (2000) 421–437.
[36] M.R.A. Blomberg, P.E.M. Siegbahn, J. Phys. Chem. B 105 (2001) 9375–9386.
[37] C.E. Cooper, Biochim. Biophys. Acta 1411 (1999) 290–309.
[38] B.A. Springer, K.D. Egeberg, S.G. Sligar, R.J. Rohlfs, A.J. Mathews, S. Olson, J. Biol. Chem. 264 (1989) 3057–3060.
[39] B.A. Springer, S.G. Sligar, J.S. Olson, J.G.N. Phillips, Chem. Rev. 94 (1994) 699–714.
[40] E. Sigfridsson, U. Ryde, J. Biol. Inorg. Chem. 4 (1999) 99–110.
[41] E. Sigfridsson, U. Ryde, J. Inorg. Biochem. 91 (2002) 101–115.
[42] C. Rovira, K. Kunc, J. Hutter, P. Ballone, M. Parrinello, J. Phys. Chem. A 101 (1997) 8914–8925.
[43] C. Rovira, K. Kunc, J. Hutter, P. Ballone, M. Parrinello, Int. J. Quantum Chem. 69 (1998) 31–35.
[44] K.P. Jensen, B.O. Roos, U. Ryde, J. Inorg. Biochem. 99 (2005) 45–54.
[45] J.N. Harvey, J. Am. Chem. Soc. 122 (2000) 12401–12402.
[46] J.N. Harvey, Faraday Discuss. 127 (2004) 165–177.
[47] S. Franzen, Proc. Natl. Acad. Sci. USA 99 (2002) 16754–16759.
[48] R. Hoffmann, M.M.-L. Chen, D.L. Thorn, Inorg. Chem. 16 (1977) 503–511.
[49] K.P. Jensen, B.O. Roos, U. Ryde, J. Inorg. Biochem, this issue; doi:10.1016/j.jinorgbio.2005.02.013.
[50] M.L. Blomberg, M.R.A. Blomberg, P.E.M. Siegbahn, J. Phys. Chem. B 107 (2003) 3297–3308.
[51] M.R.A. Blomberg, P.E.M. Siegbahn, M. Svensson, J. Chem. Phys. 104 (1996) 9546–9554.